Journal of Ceramic Processing Research. Vol. 22, No. 4, pp. 377~385 (2021)
(Received 20 June 2020, Received in revised form 22 September 2020, Accepted 2 Octobcer 2020)
https://doi.org/10.36410/jcpr.2021.22.4.377

J O U R N A L O F
Ceramic Processing Research

Thermal shock resistance of porous alumina ceramics with different internal and external porosity

Maochang Cao[a], Xinxin Jin[a,*], Le Chen[a], Limin Dong[a,b], Bo Li[c,*] and Xianyou Zhang[a]
[a]*School of Materials Science and Engineering, Harbin University of Science and Technology, Harbin 150040, P. R. China*
[b]*Key Laboratory of Engineering Dielectrics and Its Application, Ministry of Education, Harbin University of Science and Technology, 150080 Harbin, China*
[c]*Center for Precision Engineering, Harbin Institute of Technology, Harbin 150001, P.R. China*

Porous alumina ceramics with porosity of 24.42-41.10% were prepared by gel casting process with polymethylmethacrylate microsphere(PMMA) as pore-forming agent. The mechanical/thermal properties and porosity of the obtained ceramic are influenced by two structures that composed of spherical shaped micro pores(external pores) depending on PMMA content and irregular sub-micro pores(internal pores) formed by the stacking of ceramic particles. Mechanical properties and thermal conductivity decreased as the porosity increased. The thermal shock resistance of the samples was excellent when the porosity was 33.45%. This phenomenon caused by the matching of external and internal pores is inconsistent with the trend of thermal shock fracture resistance and thermal shock damage resistance varying with porosity in previous researches. In the case of the same total porosity, the introduction of external pores improved the mechanical properties and critical temperature difference, reduced the thermal conductivity and fracture surface energy that affected the thermal stability of the material.

Keywords: porous ceramics, porosity, thermal conductivity, thermal shock resistance.

Introduction

Ceramic materials are widely used in aerospace, chemical industries, petroleum and other industrial applications due to their excellent chemical stability, mechanical properties and high melting point [1-4]. However, the moderately low thermal shock resistance [5] limits its performance in a environment with rapid temperature change. To ameliorate the situation, a series of attempts and investigations were made to improve the thermal shock resistance of ceramic materials [6-10].

Recently, pores are proposed to be introduced into ceramics to improve the thermal shock properties of ceramic materials [11-13]. Coble et al. [14] analyzed the effect of pores on thermal stress in porous Al_2O_3 and predicted that the introduction of pores has a positive effect on thermal shock resistance. Other researchers [12-15] have also analyzed the effect of pores on the thermal shock resistance in porous ceramic system and confirmed that the introduction of pores had significantly improved their thermal shock resistance. This is due to the pores of ceramics, which not only passivate the crack tip to reduce the stress concentration but also promote the decrease of thermal exchange to act as the heat insulation [16]. Through X-ray diffraction analysis, it was confirmed that the pores in the specimen could effectively relieve the thermal shock stress and prevent the propagation of microcracks [17].

In later studies, ceramics with a range of porosities, were manufactured to obtain a net relation of porosity to mechanical and thermal properties [18-20]. Those investigations indicated that thermal shock fracture resistance (usually determined from the critical temperature difference, ΔT_c, for crack initiation) and thermal shock damage resistance (resistance to thermal shock crack propagation) of porous ceramics followed the typical decrease and increase with increasing porosity relationship, respectively. These conclusions about the thermal shock fracture resistance could be explained by Eq. (1), thermal shock parameter [21]:

$$R = \frac{\sigma(1-\nu)}{\alpha E} \tag{1}$$

and also be confirmed by a lot of material systems or experimental results. Therefore, the control of porosity and other pore characteristics can be used to adjust its mechanical and thermal properties, especially its thermal shock resistance.

Pores existing in the ceramics not only affect thermal shock resistance through the material properties but also through their own microstructures directly [22, 23]. Although porous ceramics with positive thermal shock resistance have be fabricated in the many investigations, the influence of porosity on the thermal shock resistance

*Corresponding author:
Tel : +86-451-86392501
Fax: +86-451-86392501
E-mail: au.zn.zn@163.com (X.-X. Jin), waymlbwd8651@126.com (B. Li)

of materials has just been preliminarily discussed, lack of in-depth researches [24]. The porosity was not further refined to analyze the dependence of external porosity on thermal shock fracture resistance and thermal shock damage resistance for the porous ceramics fabricated using pore-forming agents. Discussions on the role of the internal and external pores on thermal shock resistance of the material have hardly been reported. Thus, we also need to take into account the effect of external pores on mechanical/thermal properties and microstructures to figure out, from another perspective, how the external pores affect the thermal shock resistance.

Hence, porous Al_2O_3 ceramics were prepared by gel casting process with PMMA as pore forming agent to control the matching of external porosity (pore forming agent burning out) and internal porosity (grain natural accumulating) by changing the amount of pore forming agents. The effects of different pores matching on mechanical/thermal properties of materials were analyzed and particular emphasis was laid on thermal shock resistance. The comprehensive analysis of mechanical/thermal properties and microstructure will help to understand the influence of different pores matching on thermal shock resistance and help to further prepare ceramic materials with promising matching of thermal shock damage resistance and thermal shock fracture resistance.

Experiments

Materials

Al_2O_3 ceramic powders (>99.5% purity, D_{50} = 0.2 μm, Henan Jiyuan Brothers Materials Co., Ltd.) were used to process Al_2O_3 ceramics without pore forming agent of different porosity (28.62% and 25.84%) by agarose gel casting. 40 vol% Alumina and PMMA powder (Dongguan Baoli Mei Plastics Co., Ltd.) mixures with 10, 20, 30, 40 and 50 vol% PMMA (related to alumina powder) were dispersed in distilled water using 1 wt% agarose as binder and 0.6 wt% sodium hexametaphosphate as dispersant. The slurry was blended by ball milling for 5 h. In order to avoid the rapid evaporation of water affecting the shrinkage of the green body, it were dried at room temperature for 48h first and then at 65 ºC for 24 h. After the gelled dry green samples were moved from the mould and heated to 600 ºC for 1 h to remove the organic phases completely, it was sintered at 1600 ºC for 2 h with the heating rate of 5 ºC/min.

Characterization

Microstructures were observed by scanning electron microscopy (SEM, Hitachi SU8020). Porosity of porous ceramics was measured by Archimedes method (using deionized water as immersion fluid). Volume shrinkage was calculated according to the volume change before and after sintering. Thermal conductivity was measured using a laser thermal conductivity instrument (Model LFA 467, NETZACH, Germany). Thermal shock test of porous alumina ceramics with different porosity was performed by water quenching the specimens into a water bath (25 ºC) from higher temperature (225, 325, 425 or 525 ºC). Flexural strength and residual flexural strength were tested in three-point bending tests on 3 mm×4 mm×36 mm bars, using a 30 mm span and a crosshead speed of 0.5 mm/min. For the fracture toughness measurements, samples with 2 mm×4 mm×30 mm were loaded by a single-edge notched beam (SENB) method with a cross head speed of 0.05 mm/min.

Results and Discussion

The microstructures of porous alumina ceramics with different pore-forming agent contents are shown in Fig. 1. A dramatic increase of the spherical pore contents can be detected with the addition of 10-50 vol% (Fig. 1a-e) of PMMA. Furthermore, there are not only spherical external pores introduced by PMMA, but also internal pores formed by the stacking of ceramic particles in porous Al_2O_3 ceramics (Fig. 1f). By using Nano Measurer software, the pore size distribution range of the external pores introduced was 11-72 μm, which was more concentrated in the range of 41.5-47.6 μm. The average pore size could reach 41.33 μm. It can be seen from Fig. 1(f) that it is significantly larger than the internal pore generated by the natural accumulation of grains. For the porous alumina ceramics with different pore-forming agent contents, the average grain size (2.24 μm) and pore size almost did not change with porosity, due to the same sintering conditions. Thus, any effects on material mechanical and thermal property can be attributed to porosity and pores matching.

Fig. 2 shows the effect of different pore-forming agent contents on the porosity and volume shrinkage of materials. The black curve is the change curve of porosity with the addition of pore-forming agent. It is apparent that the porosity increased, corresponding to the porosity of 24.42%, 28.01%, 33.45%, 38.17% and 41.10%, respectively, with the increment of PMMA (10-50 vol%). When the addition of pore-forming agent was 10-40 vol%, the porosity increased about 4.5% with the addition of PMMA increased 10 vol%. When the addition of PMMA was 40-50 vol%, the porosity increased about 3% with the addition of PMMA increased 10 vol%. This is because the excessive addition of pore-forming agent caused the phenomenon of pore overlap, thus the growth rate was slower than before.

The blue curve in Fig. 2 shows that the volume shrinkage of porous alumina ceramics increased, corresponding to the shrinkage rates of 32.22%, 34.30%, 35.97%, 37.65% and 39.67%, respectively, with the addition of PMMA. On the one hand, the addition of

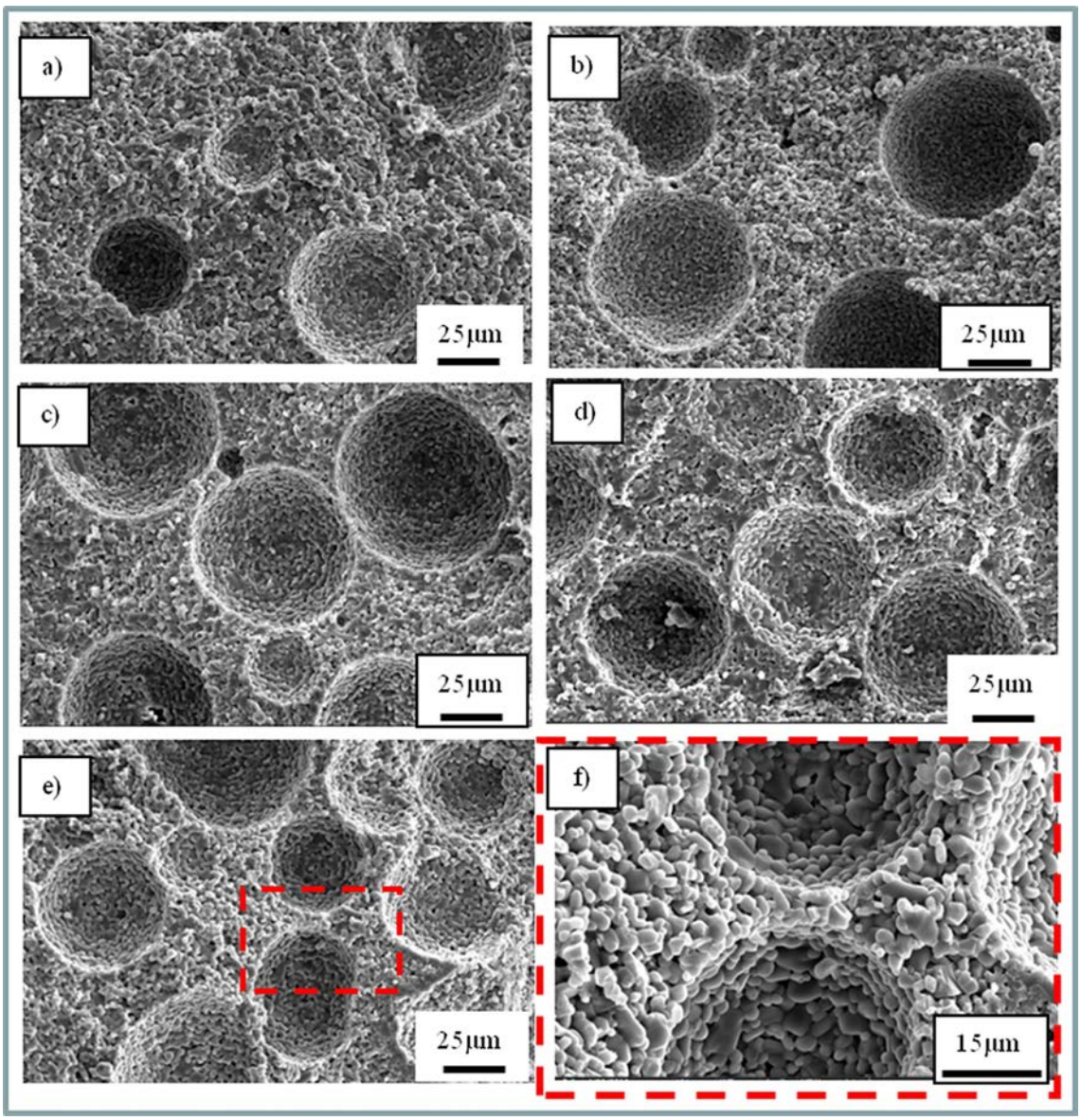

Fig. 1. SEM diagrams of porous alumina ceramics with different pore-forming agent contents. The SEM maps of porous alumina with 10, 20, 30, 40 and 50 vol% pore-forming agent content are (a), (b), (c), (d) and (e) respectively, and (f) a local enlargement of figure (e).

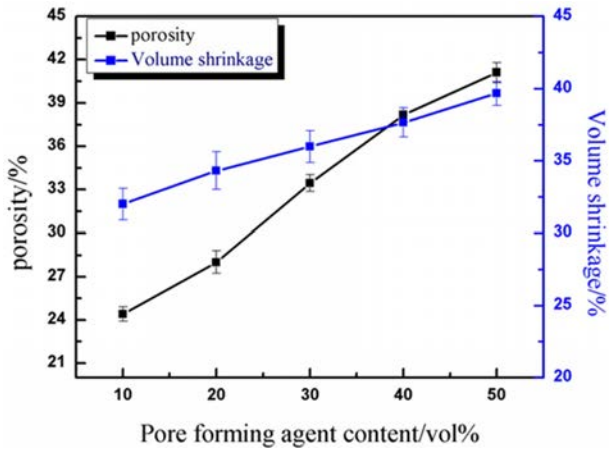

Fig. 2. Effect of different pore forming agent contents on porosity and volume shrinkage.

pore-forming agent led to the increase of the effective solid content of slurry, which might result in the decrease of volume shrinkage; on the other hand, the addition of pore-forming agent left large pore in the matrix, which shrank during sintering process, leading to the increase of volume shrinkage [25]. Obviously, the latter played a decisive role in this article. With the increase of the addition of pore-forming agent, volume shrinkage increased linearly. With the addition of PMMA increased 10 vol%, the volume shrinkage increased about 1.86%.

So as to research the effect of pores matching on the properties of materials, the internal and external pores of materials with different pore-forming agent addition were estimated. Based on the experimental results [26, 27], the following assumptions are made: (i) the shrinkage of internal pores is not affected by external pores.

Internal porosity depends on the effective solid content. (ii) When the effective solid content was the same, the shrinkage caused by sintering of powder particles at the same sintering conditions remained the same. With those assumption, the internal and external porosity can be calculated using the following equation:

$$P_t = P_e + P_i \quad (2)$$

Where P_t is total porosity, P_e is external porosity, P_i is internal porosity, the matching of internal and external porosity of porous alumina ceramics with different addition of pore-forming agent are shown in Fig. 3.

Fig. 3 gives the matching distribution of internal and external pore of porous alumina ceramics with different PMMA contents. The black curve is the change curve of the total porosity with the addition of PMMA and the red curve is the change curve of the external porosity with the addition of PMMA. The external porosity increased, corresponding to the porosity of 3.4%, 10.54%, 19.28%, 27.14% and 33.09%, respectively, with the increment of PMMA (10-50 vol%) and the porosity increased about 7.42% with the addition of PMMA increased 10 vol%.

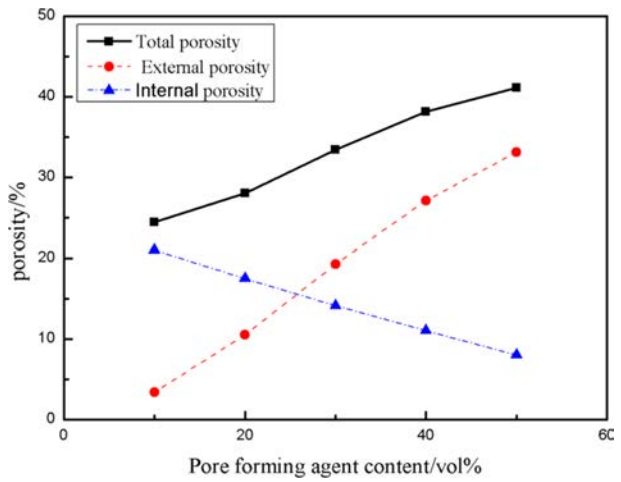

Fig. 3. Pore matching distribution of porous alumina ceramics with different pore-forming agent contents.

The blue curve is the change curve of internal porosity with the addition of PMMA. The internal porosity decreased, corresponding to the porosity of 21.02%, 17.47%, 14.17%, 11.03% and 8.01%, respectively, with the increment of PMMA (10-50 vol%) and the porosity decreased about 3.25% with the addition of PMMA increased 10 vol%. The decrease of internal porosity indicates that the contact area between grains increases.

Fig. 4 shows the effect of different porosity on the flexural strength of porous alumina ceramics without pore-forming agent addition and with different contents of pore-forming agents. The total porosity of porous alumina ceramics with pore-forming agent addition ranges from 24.42% to 41.10%, corresponding to the flexural strength of 116.40, 107.54, 98.38, 93.14 and 88.69 MPa, respectively. The flexural strength of these groups both decreased with increasing porosity. In the case of similar total porosity, the introduction of external pores led to the increase of the effective solid content of the material, which made the internal porosity decrease relatively, increasing the contact between grains, and improving theflexural strength of the samples.

Elastic modulus is a physical quantity describing the ability of material to resist deformation. The effect of different porosity on elastic modulus of material is shown in Fig. 5. As can be seen from Fig. 5, the variation of elastic modulus with porosity is as follows: with the increase of porosity, the elastic modulus decreases gradually and the attenuation trend decreases gradually. The elastic modulus of samples with different porosity are 74.81, 60.56, 50.41, 45.51 and 42.77 GPa, respectively. That conforms to the exponential trend [28].

Through fitting for the ceramics with different contents of pore-forming agents, the elastic modulus of the sample conformed to the formula: E = 155.92

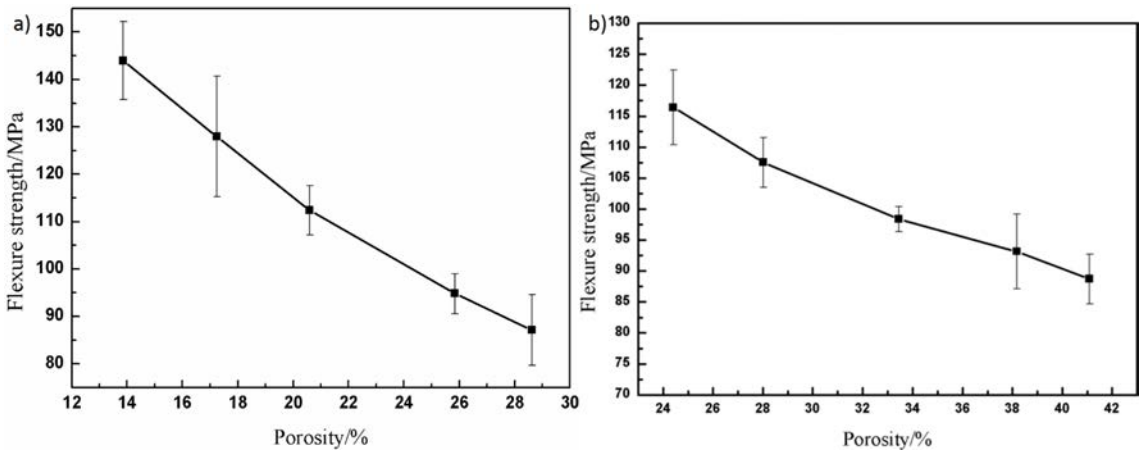

Fig. 4. Effect of porosity on flexure strength of porous Al_2O_3 ceramics: (a) without pore-forming agents; (b) with different contents of pore-forming agents.

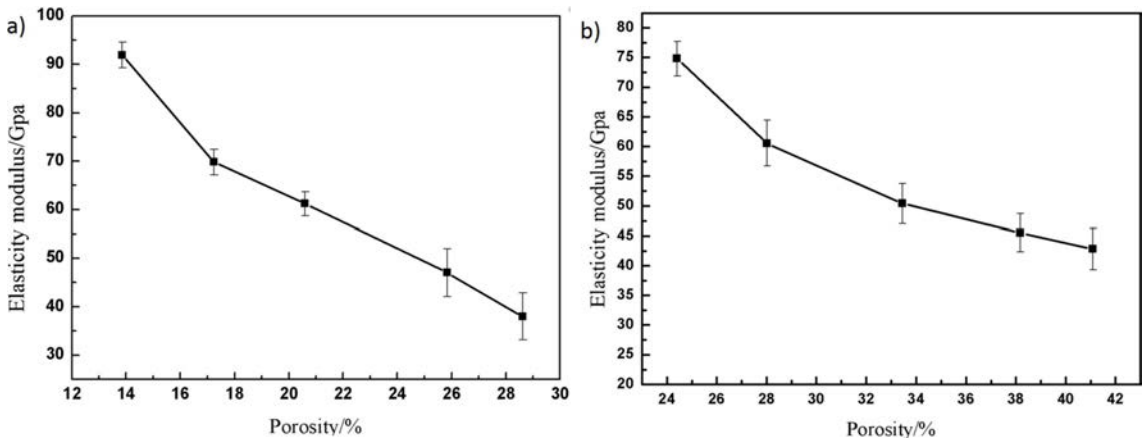

Fig. 5. The relationship between porosity and elasticity modulus: (a) without pore-forming agents; (b) with different contents of pore-forming agents.

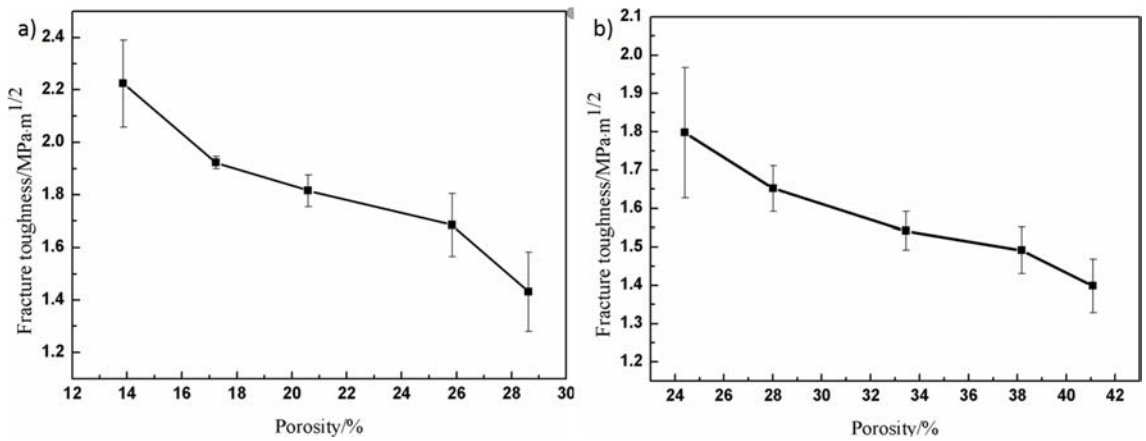

Fig. 6. The relationship between porosity and fracture toughness of porous alumina ceramics: (a) without pore-forming agents; (b) with different contents of pore-forming agents.

exp(-3.2*P*), $R^2 = 0.96$. Comparing with the fitting formula of flexural strength, it is found that the dependence of elastic modulus on porosity is greater than that of flexural strength on porosity. The different dependence may affect the damage tolerance and the release rate of elastic strain energy, which may affect the crack growth and propagation under the action of thermal stress. Moreover, by comparing the elastic modulus of the samples with that of the ceramics without pore-forming agents but with the similar total porosity, it is found that the introduced external pores increased the elastic modulus obviously.

Fig. 6 shows the relationship between different porosity and fracture toughness of porous alumina ceramics. The fracture toughness of samples decreases with the increase of porosity. When the porosity is 38.17-41.10%, the fracture toughness decreases slightly, the reason of which may be that with the increase of pore-forming agent, the introduced external holes overlapped in the sample, which accelerated the decrease of material strength. Fracture toughness is related to material strength and critical crack size as shown in Eq. (2), in which the strength of ceramics decreases with the increase of porosity and the critical crack size increases with the increase of porosity [29]. Therefore, with the increase of porosity, the fracture toughness decreases gradually, probably because the strength of ceramics decreases more than the critical crack size of ceramics, which leads to the decrease of fracture toughness. Moreover, comparing the Fig. 6(a) and Fig. 6(b), a slight improvement was found in the fracture toughness due to the introduction of the external pores.

$$a_{cr} = \frac{K_{IC}^2}{\pi \sigma_f^2} \tag{2}$$

Where a_{cr} is the critical crack size, K_{IC} is fracture toughness, σ_f is the flexural strength.

Novais et al. [30] prepared porous alumina ceramics with different pore gradient distribution using polypropylene (PP) and polymethylmethacrylate (PMMA) as pore-forming agents. The experimental results shown that the thermal conductivity can be adjusted according to the volume and size of the generated pore, thus that the material properties can be adjusted according to the anticipated application. In this experiment, by changing

the amount of pore-forming agent, we can control the pore gradation of the material's external and internal holes and then control the micro-structure and change the thermal conductivity.

Fig. 7 shows the relationship between porosity and thermal conductivity at room temperature and 500 ºC. The thermal conductivity decreased with the increase of porosity. The black line is the variation curve of thermal conductivity with porosity at room temperature. At 27 ºC, the total porosity was 24.42-41.10% and the thermal conductivity was 14.02-10.35 W/(m·K). The change curve of thermal conductivity with porosity at 500 ºC was 24.42-41.10% in total porosity and 5.63-4.41 W/(m·K) in thermal conductivity.

Previous experiments in which thermal conductivity decreased monotonously with the increase of porosity [30]. According to the expression formula of thermal conductivity of porous alumina ceramics [31]:

$$\lambda = \lambda_s M(1-P)^{3/2} + \lambda_p P^{1/4} \quad (3)$$

Among them, λ_s is the thermal conductivity of compact materials; M is the influence value of defects in materials, which is inversely proportional to crack size and grain spacing, and directly proportional to the contact area between grains [32], P is the total porosity of porous materials; λ_p is the thermal conductivity of gases in holes.

On the one hand, the increase of the amount of pore-forming agent led to the increase of external pore (pore size is less than 100 μm, without considering convective transfer [33]), which prevented heat transfer; on the other hand, the internal porosity of the material decreased, grain spacing decreased and the contact area between grains increased, thus the M value increased accordingly. With the increase of total porosity P, $(1\text{-}P)^{3/2}$ decreased and $p^{1/4}$ increased. The thermal conductivity of materials decreased with the increase of total porosity under the synergistic effect of internal pore and external pore, i.e. M and P, indicating that the influence of external pore on thermal conductivity of materials was dominant.

Molecular motion theory model of phonon thermal conductivity of crystal material given by Debye [34]:

$$\lambda_s = \frac{1}{3} C\bar{v}l \quad (4)$$

Among them, C is the volume heat capacity of phonons, $\bar{v}$ is the average velocity of phonons, and l is the average free path of phonons. When a certain temperature is reached (500 ºC, without considering radiation transfer), the average free path of phonon decreased with the increase of temperature, thus the thermal conductivity decreased with the increase of temperature. Besides, comparing the results in Fig. 7(a) and Fig. 7(b), the external big and spherical pores was proved to be unfavorable to the heat transfer of the material, thus reducing the thermal conductivity.

Fig. 8 shows the flexural strength of porous alumina ceramics with different porosity varying with thermal shock temperature. The five broken lines represent the variation of flexural strength of porous alumina ceramics with porosity of 24.42%, 28.01%, 33.45%, 38.17% and 41.10%, respectively. As can be seen from Fig. 8, the flexural strength of alumina ceramics with the same porosity decreased gradually with the increase of thermal shock temperature difference. Under the same thermal shock temperature difference, the flexural strength decreased with the increase of porosity.

Critical temperature difference refers to the temperature difference corresponding to the ratio of residual strength to initial strength of materials after thermal shock at 70%. The greater the critical temperature difference is, the better the thermal shock fracture resistance is. The critical temperature differences of 24.42%, 28.01%, 33.45%, 38.17% and 41.10% porosity are 367, 373, 386, 350 and 320 ºC, respectively. With the increase of

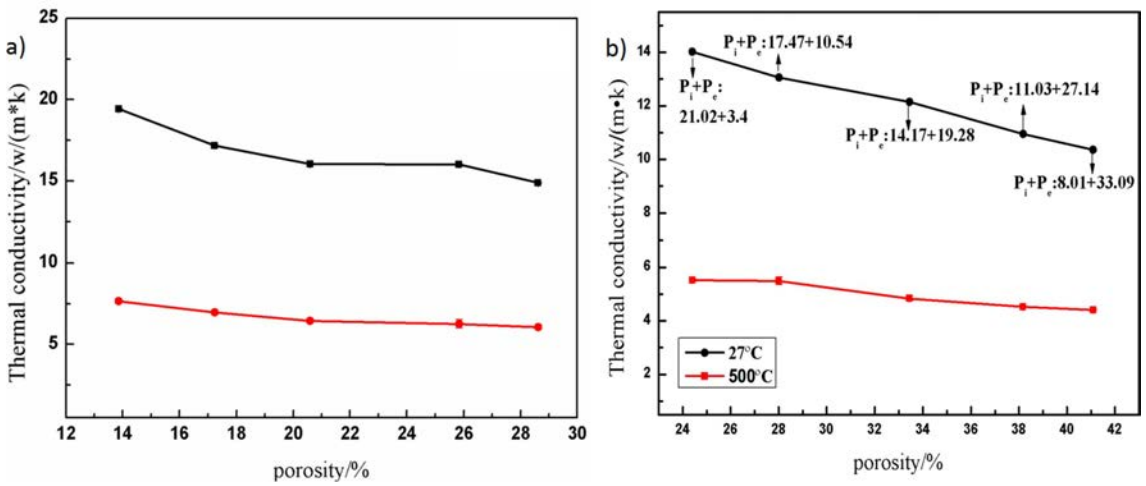

Fig. 7. The relationship between porosity and thermal conductivity at different temperatures: (a) without pore-forming agents; (b) with different contents of pore-forming agents.

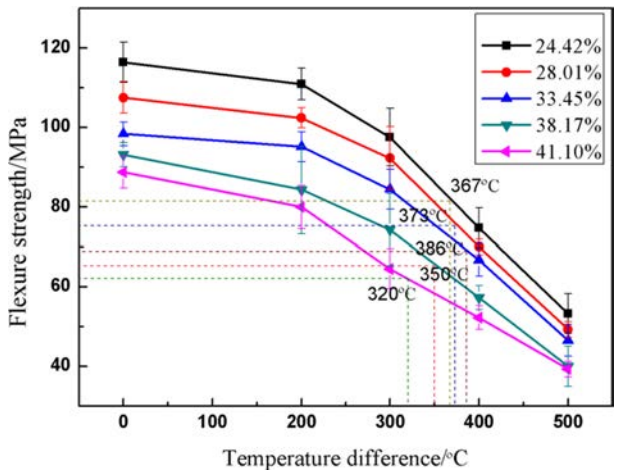

Fig. 8. The variation of flexural strength with thermal shock temperature difference of alumina ceramics with different porosity.

porosity, it shows a trend of first increasing and then decreasing. Unlike the theoretical critical temperature difference, it decreases with the increase of porosity. According to Eq. (5), the relationship between the ultimate strength and the critical temperature difference of the material is as follows:

$$\Delta T = R'S \times \frac{1}{0.31 r_m h} = \frac{\sigma_f \lambda (1-\nu)}{\alpha E} S \times \frac{1}{0.31 r_m h} \tag{5}$$

Among them, R' is called the second thermal stress fracture resistance factor, σ_f is the ultimate strength of the material, r_m is the effective thickness of the specimen and h is the heat transfer coefficient of the sample. The critical temperature difference is proportional to the ultimate strength and thermal conductivity of the material and inversely proportional to the elastic modulus. Set $(1-\nu)/\alpha$ as the constant a and brought in the numerical value. The results of different porosity were as follows: 21.81a, 23.19a, 23.74a, 22.41a and 21.46a. The calculated results were in excellent agreement with the experimental results. When the porosity was 33.45%, the thermal shock fracture resistance was the best and the critical temperature difference was 386 °C.

The h of the sample is inversely proportional to the critical temperature difference, which has an important influence on the thermal stability of the sample [35]. However, the accurate measurement of the heat transfer coefficient is a difficult problem. Therefore, we measure the contact angle between the sample and the quenching medium. According to the Fig. 9 the contact angle between the samples with different porosity and the quenching medium, when the porosity is 24.42-41.10%, the contact angles are 108.5°, 110.2°, 134.6°, 111.3° and 109.7°, respectively, which are >90°. According to Eq. (6):

$$S'/S = n\pi l'^2 / n\pi l^2 = r^2 \sin^2(\pi - \theta)/r^2 = \sin^2\theta \tag{6}$$

Where S' is the contact area between the quenching medium and the sample in unit area; S is the unit area when the quenching medium completely contacts the sample; n is the number of water drops in unit area; r is the radius of water drops; and θ is the contact angle. When the θ changes, it means that the contact area between the quenching medium and the sample surface is changing, which will affect the heat transfer between the material surface and the quenching medium and then affect the value of h. With the increase of porosity,

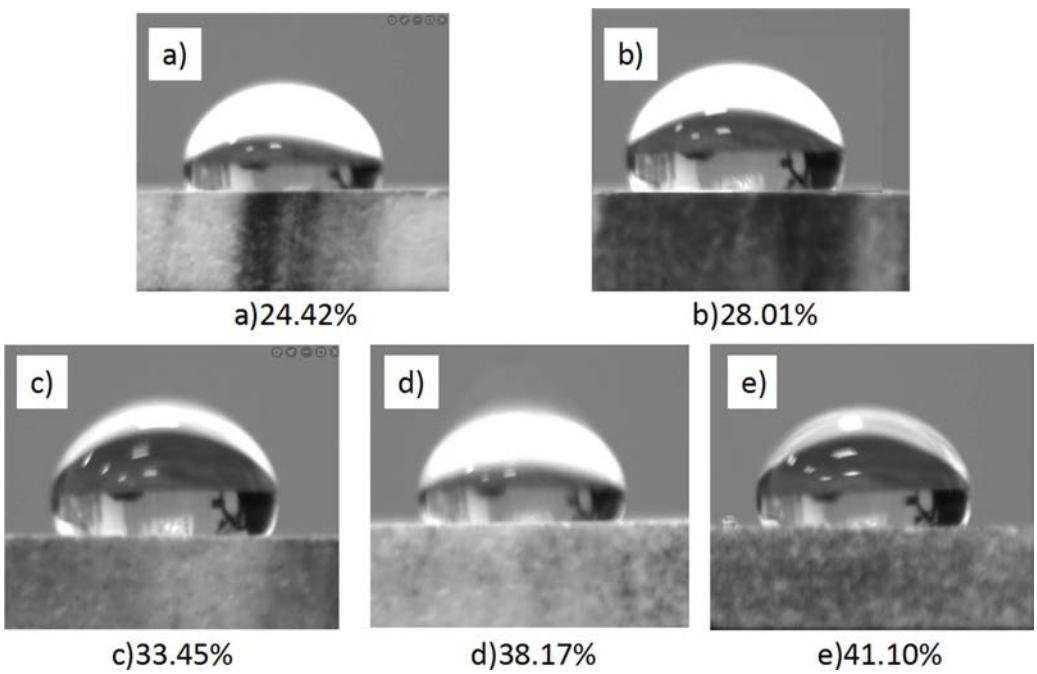

Fig. 9. Contact angle measurement of different porosity.

the θ between the sample and the quenching medium tends to decrease. However, when the porosity is 33.45%, the θ is greatly increased, which will affect the h of the material and increase the ΔT.

Residual strength retention ratio represents the ratio of the strength of ceramic materials after thermal shock to the initial strength of ceramic materials, which can be used to characterize the thermal shock damage resistance of materials. Under the thermal shock temperature difference of 500 °C, the residual strength retention rates of 24.42-41.10% of the porosity were 45.77%, 45.80%, 47.28%, 42.94% and 44.23%, respectively. The thermal shock damage resistance of materials increased firstly and then decreased. According to Eq. (7) of fracture surface energy, the calculated fracture surface energies were 21.59, 22.53, 23.57, 23.11 and 22.84 $J \cdot m^{-1}$, respectively.

$$\gamma = \frac{K_{IC}^2}{2E} \tag{7}$$

As Yuan et al. [12] found, the fracture surface energy of the material increased firstly and then decreased with the increase of porosity, which may be due to the bridging effect of pore [36]. Under thermal shock condition, the fracture surface energy consumed by crack propagation is large, the extent of crack propagation is small, and the thermal stability of materials is excellent. Therefore, the thermal shock damage resistance of materials is proportional to the fracture surface energy. The experimental results were in agreement with the results. When the porosity was 33.45%, the thermal shock damage resistance of the material was the superior.

Conclusion

Porous alumina ceramics with different distribution of external pores and internal pores were fabricated using gel-casting with adding pore forming agents. Research herein is mainly focused on the effects of different pore gradations on the mechanical properties and thermal properties:

(1) The flexural strength and modulus of elasticity decreased exponentially with the increase of porosity and the dependence of elastic modulus on porosity was greater than that of flexural strength on porosity.

(2) The external pores improved the mechanical properties of the porous alumina ceramic: the strength and elastic modulus of the materials were both improved, and the fracture toughness was also improved by a small extent, but they were not conducive to heat transfer and reduced the thermal conductivity of the materials.

(3) The critical temperature difference increased first and then decreased with the increased of porosity. Because of the matching of internal and external pore affected the change trend of thermal conductivity. The influence of external porosity on thermal conductivity was dominant.

(4) The thermal shock damage resistance was proportional to the fracture surface energy affected by pore matching, which increased firstly and then decreased.

Acknowledgments

This work was financially supported by the National Natural Science Foundation of China (Nos. 51602082) and Heilongjiang Province Colleges and universities Youth Innovation Talents Training Program (Nos. UNPYSCT-2017083).

References

1. X.H. Xu, X.Y. Xu, J.F. Wu, Y. Zhou, and D.Z. He, Appl. Mech. Mater. 692 (2014) 217-223.
2. E.P. Simonenko, D.V. Sevast'Yanov, N.P. Simonenko, V.G. Sevast'yanov, and N.T. Kuznetsov, Russ. J. Inorg. Chem. 58 (2013) 1669-1693.
3. R. Kelling, G. Eigenberger, and U. Nieken, Catal. Today. 273 (2016) 196-204.
4. J.H. Lee, J.II. Youn, Y.J. Kim, I.K. Kim, K.W. Jang, and H.J. Oh, Ceram. Int. 41[9] (2015) 11899-11907.
5. D.P.H. Hasselman, J. Am. Ceram. Soc. 52[11] (1969) 600-604.
6. Z.H. Wu, W.D. Liu, and L.C. Zhang, J. Am. Ceram. Soc. 101[8] (2018) 3583-3596.
7. M. Rühle, N. Claussen, and A.H. Heuer, J. Am. Ceram. Soc. 69[3] (1986) 195-197.
8. L. Silvestroni, D. Sciti, C. Melandri, and C. Guicciardi, J. Eur. Ceram. Soc. 30[11] (2010) 2155-2164.
9. Y. Kim, C.S. Jang, J.W. Choi, and E. Kim. J. Ceram. Process. Res. 15[5] (2014) 277-280.
10. E. Srinivasa Rao and P. Manohar, J. Ceram. Process. Res. 17[11] (2016) 1164-1170.
11. L.T. Wei, Y.H Yu, and J. Jiao, J. Ceram. Process. Res. 19[2] (2018) 126-129.
12. C. Yuan, L.J. Vandeperre, R.J. Stearm, and W.J. Clegg, J. Mater. Sci. 43[12] (2008) 4099-4106.
13. X.X. Jin, L.M. Dong, H.Y. Xu, L.Z. Liu, N. Li, X.H. Zhang, and J.C. Han, J. Ceram. Int. 42[7] (2016) 9051-9057.
14. R.L. Coble and W.D. Kingery, J. Am. Ceram. Soc. 38[1] (1955) 33-37.
15. Y.F. Shao, R.Q. Du, X.F. Wu, F. Song, X.H. Xu, and C.P. Jiang, J. Mater. Sci. 48[18] (2013) 6431-6436.
16. Y.L. Dong and W.M. Wang, J. Adv. Ceram. 25[1] (2004) 37-41.
17. L.Y. Shen, M.J. Liu, X.Z. Liu, and B. Li, Mater. Res. Bull. 42[12] (2007) 2048-2056.
18. J.H. She, J.F. Yang, and T. Ohji, J. Mater. Sci. Lett. 22[5] (2003) 331-333.
19. V. Sciamanna, B. Nait-Ali, and M. Gonon, J. Ceram Int. 41[2] (2015) 2599-2606.
20. X.X. Jin, L.M. Dong, H.Y. Xu, L.Z. Liu, N. Ling, X.H. Zhang, and J.C. Han, Ceram. Int. 42[7] (2016) 9051-9057.
21. J.W. Zimmermann, G.E. Hilmas, and W.G. Fahrenholtz, Mater. Chem. Phys. 112[1] (2008) 140-145.
22. S. Li, C.A. Wang, and J. Zhou, Ceram. Int. 39[8] (2013) 8833-8839.

23. K. Mohanta, A. Kumar, O. Parkash, and D. Kumar, J. Am. Ceram. Soc. 97[6] (2014) 1708-1719.
24. K. Moritz and C.G. Aneziris, Ceram. Int. 42[12] (2016) 14155-14160.
25. S.T. Lin and R.M. German, J. Am. Ceram. Soc.71[10] (1988) C432-433.
26. H.X. Shang, A. Mohanram, and R.K. Bordia, J. Am. Ceram. Soc. 98[11] (2015) 3424-3430.
27. E. Gregorová and W. Pabst, J. Am. Ceram. Soc. 31[12] (2011) 2073-2081.
28. W. Pabst, E. Gregorová, and G. Tichá, J. Am. Ceram. Soc. 26[7] (2006) 1085-1097.
29. C. Aksel and P.D. Warren, J. Eur. Ceram. Soc. 23[2] (2003) 301-308.
30. R.M. Novais, M.P. Seabra, and J.A. Labrincha, Ceram. Int. 40[8] (2014) 11637-11648.
31. E.Y. Litovsky, M. Shapiro, and A. Shavit, J. Am. Ceram. Soc. 79[5] (2010) 1366-1376.
32. E.Y. Litovsky and M. Shapiro, J. Am. Ceram. Soc. 75[12] (1992) 3425-3439.
33. K. Mohanta, A. Kumar, O. Parkash, and D. Kumar, J. Am. Ceram. Soc. 97[6] (2014) 1708-1719.
34. S.W. Yuan, Y.H. Feng, X. Wang, and X.X. Zhang, Acta Phys. Sin. (Chinese Ed.) 63[1] (2014) 014402.
35. F. Song, S.H. Meng, X.H. Xu, and Y.F. Shao, Phys. Rev. Lett. 104[12] (2010) 125502.
36. R.W. Rice, J. Mater. Sci. 31[8] (1996) 1969-1983.